Supplementary Information

Pharmacological Blockade of NMUR2 Suppresses Glioma Growth by Inhibiting STAT5-Mediated Transcription of Cell Cycle-associated Genes

Yuna Roh, Taesang Son, Tae-Hee Han, Sarang Kim, Eunsun Jung, Jin-Seong Hwang, Joo-Young Im, Mi-Jung Kang, Mun Jeong Cho, Jung Hwa Lim, Cho-Rok Jung, Moo-Seung Lee, Hyun-Soo Cho, Dae-Soo Kim, Mi-Young Son, Seon-Young Kim, Seon-Kyu Kim*, Hyun Seung Ban*, Jang-Seong Kim* and Tae-Su Han*

***Corresponding authors:**

Tae-Su Han, Biotherapeutics Translational Research Center, Korea Research Institute of Bioscience and Biotechnology, 125 Gwahak-ro, Yuseong-gu, Daejeon 34141, Republic of Korea. Phone: +82-42-860-4297; E-mail: tshan@kribb.re.kr

Jang-Seong Kim, Biotherapeutics Translational Research Center, Korea Research Institute of Bioscience and Biotechnology, 125 Gwahak-ro, Yuseong-gu, Daejeon 34141, Republic of Korea. Phone: +82-42-860-4001; E-mail: jangskim@kribb.re.kr

Hyun Seung Ban, Biotherapeutics Translational Research Center, Korea Research Institute of Bioscience and Biotechnology, 125 Gwahak-ro, Yuseong-gu, Daejeon 34141, Republic of Korea. Phone: +82-42-879-8176; E-mail: banhs@kribb.re.kr

Seon-Kyu Kim, Aging Convergence Research Center, Korea Research Institute of Bioscience and Biotechnology, 125 Gwahak-ro, Yuseong-gu, Daejeon 34141, Republic of Korea. Phone: +82-42-879-8107; E-mail: seonkyu@kribb.re.kr

Supplementary Figures

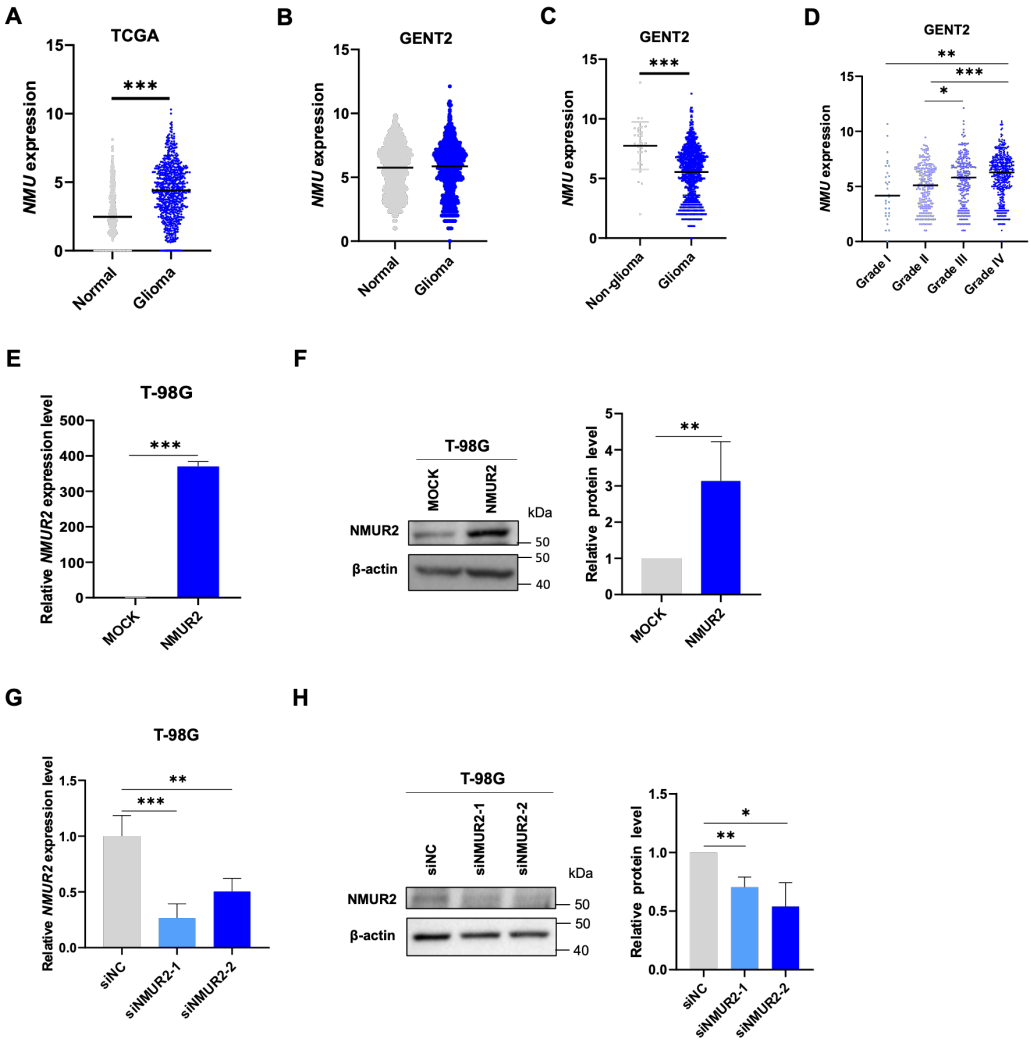

Figure S1. NMU expression in glioma datasets and NMUR2 expression in T-98G cells following overexpression or knockdown.

A. *NMU* expression in human normal brain tissues (n = 1141) and glioma tissues (LGG + GBM, n = 689) based on TCGA dataset analysis. B-D. *NMU* expression analysis using the GENT2 database. B. Comparison of *NMU* expression between normal brain tissues (n = 873) and glioma tissues (n = 946). C. Comparison of *NMU* expression between non-glioma brain tumor samples (n = 32) and glioma tissues (n = 946). D. *NMU* expression according to glioma grade. E-F. NMUR2 expression in T-98G cells transfected with empty vector or NMUR2 expression vector. E. *NMUR2* mRNA expression determined by qPCR. F. NMUR2 protein expression determined by western blotting. G-H. *NMUR2* expression in T-98G cells transfected with siNC or siNMUR2. G. *NMUR2* mRNA expression determined by qPCR. H. NMUR2 protein expression determined by western blotting. Data are presented as means ± SD (**P* < 0.05, ***P* < 0.01, ****P* < 0.001).

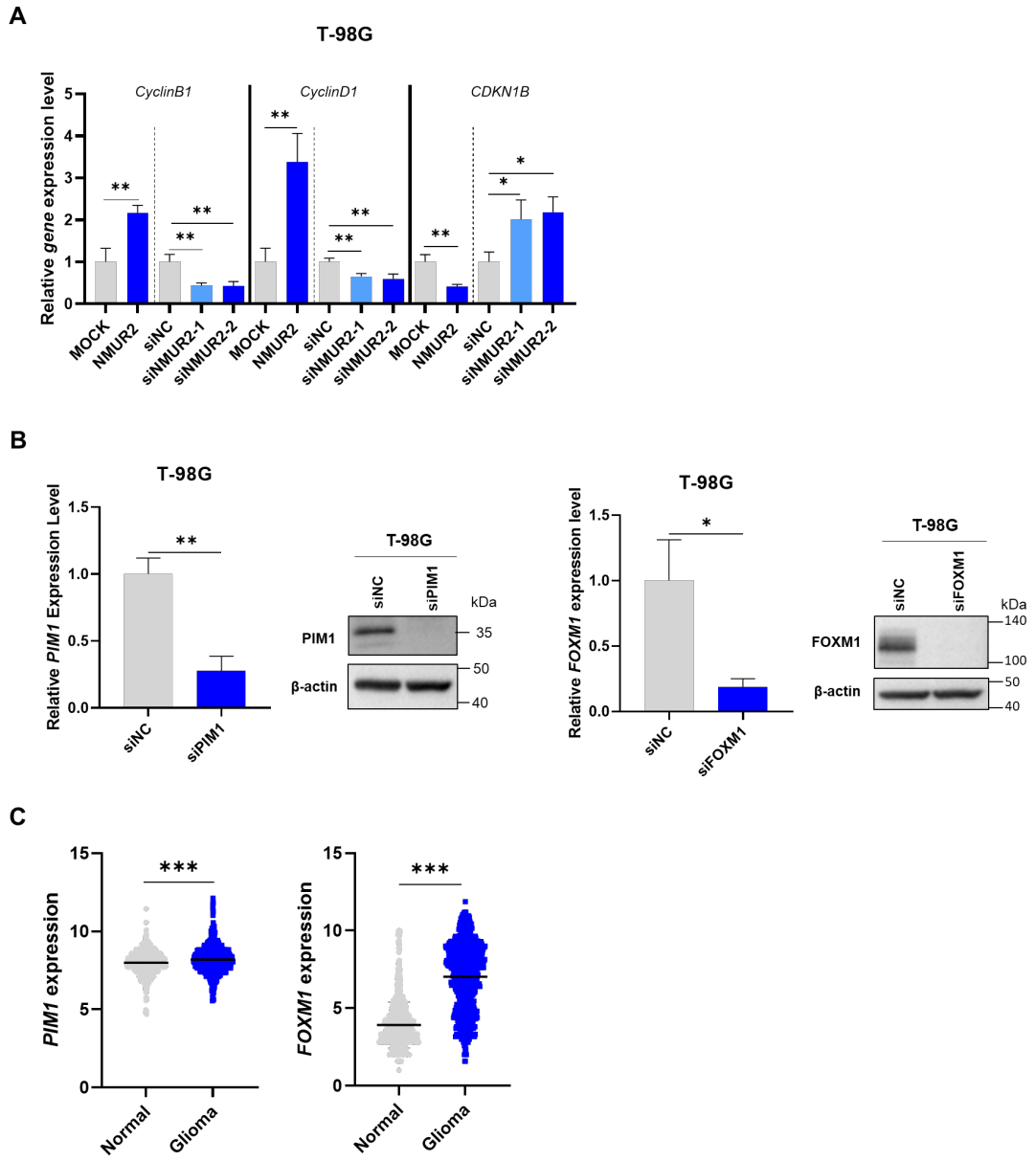

Figure S2. NMUR2 expression is involved in the regulation of the cell cycle.

A. The mRNA expression levels of *CyclinD1* and *CyclinB1* (cell cycle progression genes) and *CDKN1B* (a cell cycle repression gene) were analyzed using RT-qPCR in T-98G cells with NMUR2 overexpression or knockdown. B. PIM1 and FOXM1 expression in T-98G cells transfected with siNC, siPIM1, or siFOXM1. mRNA expression was determined by RT-qPCR, and protein expression was determined by western blotting. C. *PIM1* (left) and *FOXM1* (right) expression in human normal brain tissues (n = 873) and glioma tissues (n = 946) based on GENT2 database analysis (http://gent2.appex.kr/gent2/). Data are presented as means ± SD (*$P < 0.05$, **$P < 0.01$, ***$P < 0.001$).

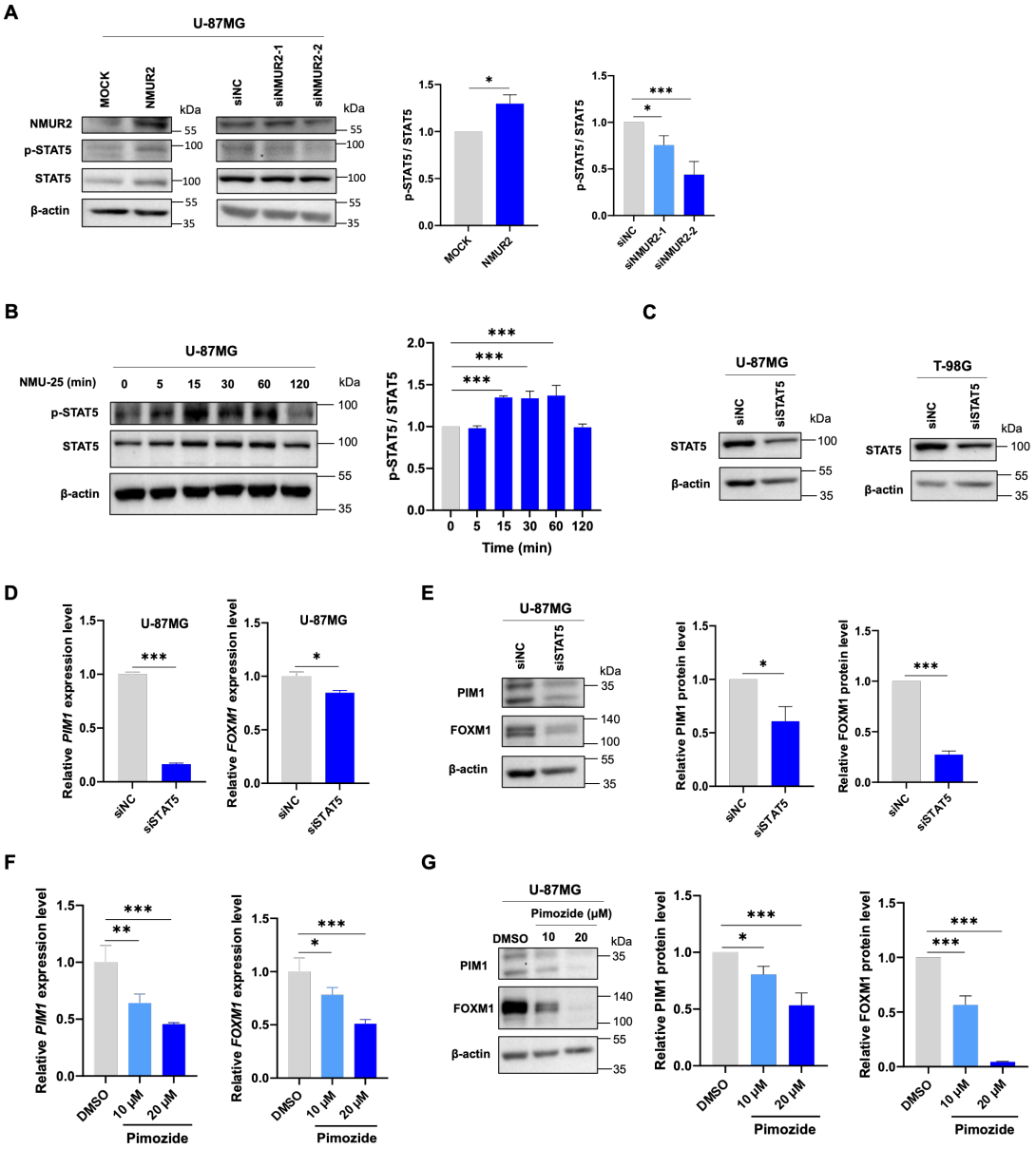

Figure S3. NMUR2-associated STAT5 activation and STAT5-dependent regulation of PIM1 and FOXM1 expression in glioma cells.

A. Phospho-STAT5 and total STAT5 levels in U-87MG cells following NMUR2 overexpressio n or knockdown, determined by western blotting. B. Time-dependent phosphorylation of STAT5 in U-87MG cells following NMU-25 treatment (0, 5, 15, 30, 60, and 120 min), determined by western blotting. Phospho-STAT5 levels were quantified relative to total STAT5. C. STAT5 protein expression in U-87MG and T-98G cells transfected with non-targeting control siRNA (siNC) or STAT5-targeting siRNA (siSTAT5), determined by western blotting. D-E. PIM1 and FOXM1 expression in U-87M G cells following siRNA-mediated STAT5 knockdown. D. *PIM1* and *FOXM1* mRNA expressi on determined by RT-qPCR. E. PIM1 and FOXM1 protein expression determined by western

blotting. F-G. PIM1 and FOXM1 expression in U-87MG cells treated with the indicated conc entrations of Pimozide. F. *PIM1* and *FOXM1* mRNA expression determined by RT-qPCR. G. PIM1 and FOXM1 protein expression determined by western blotting. Data are presented as means ± SD (*$P < 0.05$, **$P < 0.01$, ***$P < 0.001$).

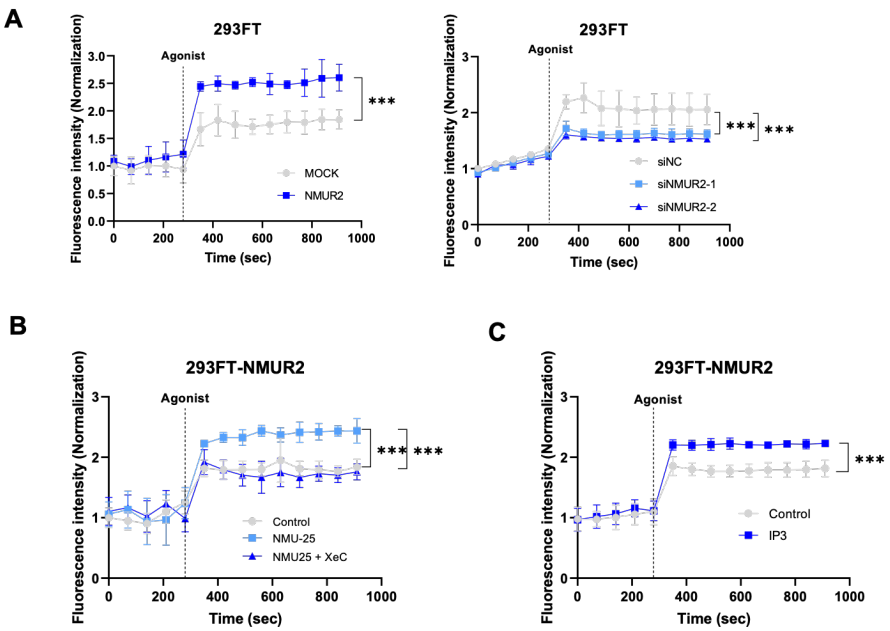

Figure S4. Intracellular Ca^{2+} analysis in 293FT cells following modulation of NMUR2 signaling.

A-C. Intracellular Ca^{2+} levels in 293FT cells measured using Green FLUOFORTE Dye. A. Intracellular Ca^{2+} levels in 293FT cells following NMUR2 overexpression or knockdown. B. Intracellular Ca^{2+} levels in 293FT cells treated with NMU-25 and Xestospongin C. C. Intracellular Ca^{2+} levels in 293FT cells treated with IP3. Data are presented as means ± SD (***$P < 0.001$).

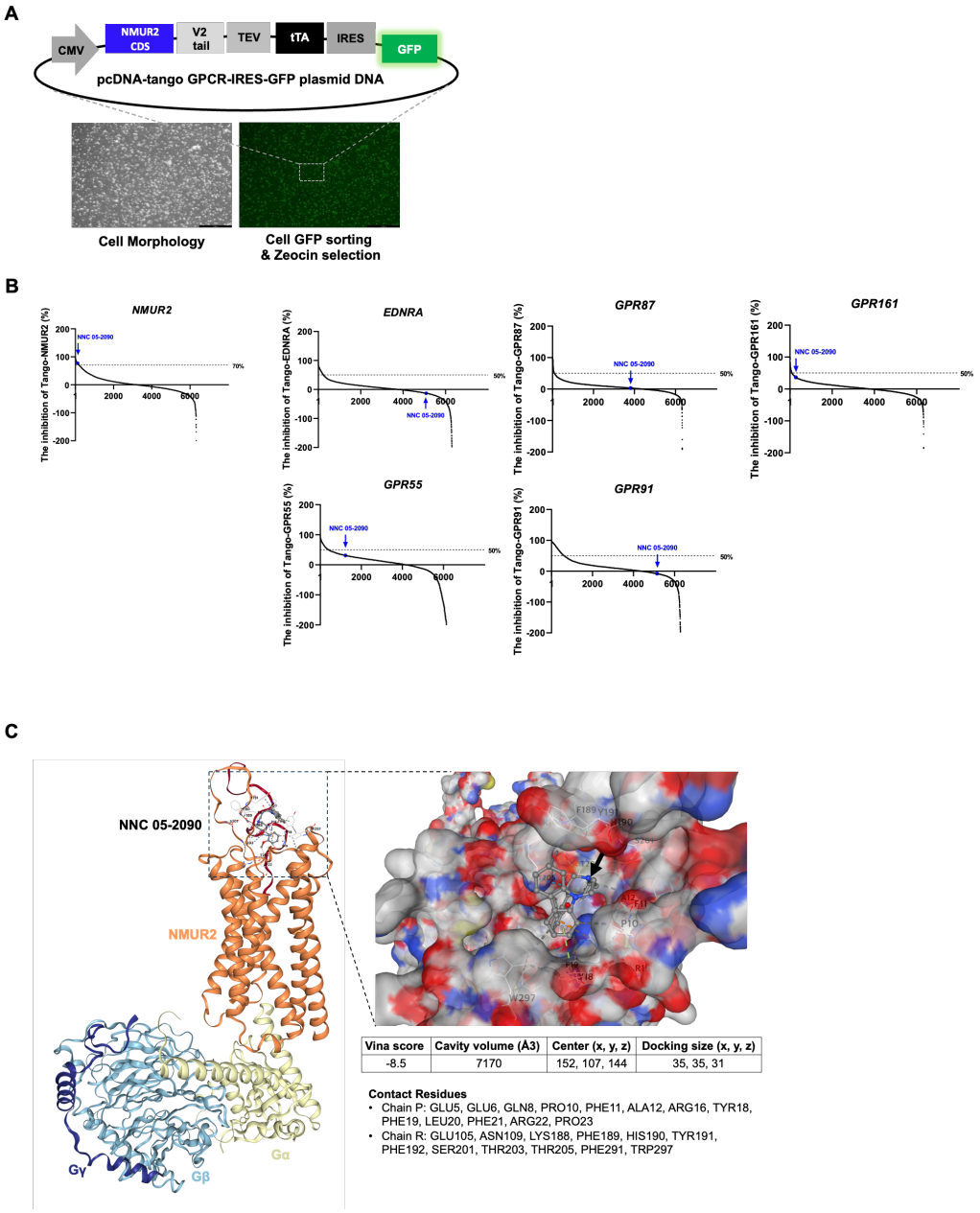

Figure S5. Construction of the NMUR2-specific PRESTO-TANGO screening system and evaluation of NNC 05-2090 selectivity.

A. Schematic representation of the pIRES-EGFP-NMUR2 plasmid and validation of the stable HTLA-NMUR2 cell line expressing GFP. The optimized NMUR2 TANGO coding sequence was inserted into the coding region of the pIRES-EGFP vector derived from the pcDNA3.1 backbone. B. Inhibition rates of NNC 05-2090 in NMUR2 and other GPCR assays. Luciferase inhibition rates were used to evaluate compound activity across receptors. C. Representative docking model of NNC 05-2090 in NMUR2 generated using CB-Dock2 with the NMUR2 structure (PDB ID: 7XK8). The predicted binding pocket is shown with the docked ligand, together with the corresponding vina score (-8.5 kcal/mol) and cavity volume (7170) obtained from CB-Dock2.

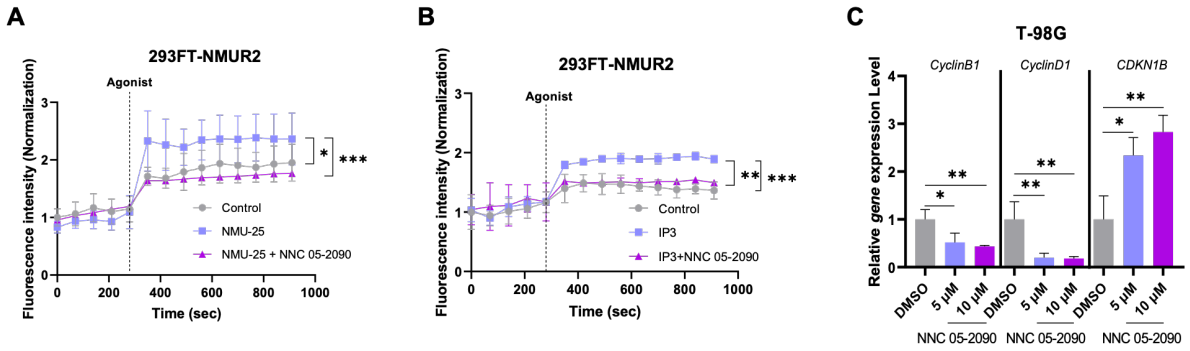

Figure S6. Intracellular Ca^{2+} analysis and cell cycle-associated gene expression following NNC 05-2090 treatment.

A-B. Intracellular Ca^{2+} levels in 293FT cells measured using Green FLUOFORTE Dye. A. Intracellular Ca^{2+} levels in cells treated with NMU-25 or co-treated with NMU-25 and NNC 05-2090. B. Intracellular Ca^{2+} levels in cells treated with IP3 or co-treated with IP3 and NNC 05-2090. C. *Cyclin B1*, *Cyclin D1*, and *CDKN1B* mRNA expression in T-98G cells treated with the indicated concentrations of NNC 05-2090, determined by RT-qPCR. Data are presented as means ± SD (*$P < 0.05$, **$P < 0.01$, ***$P < 0.001$).

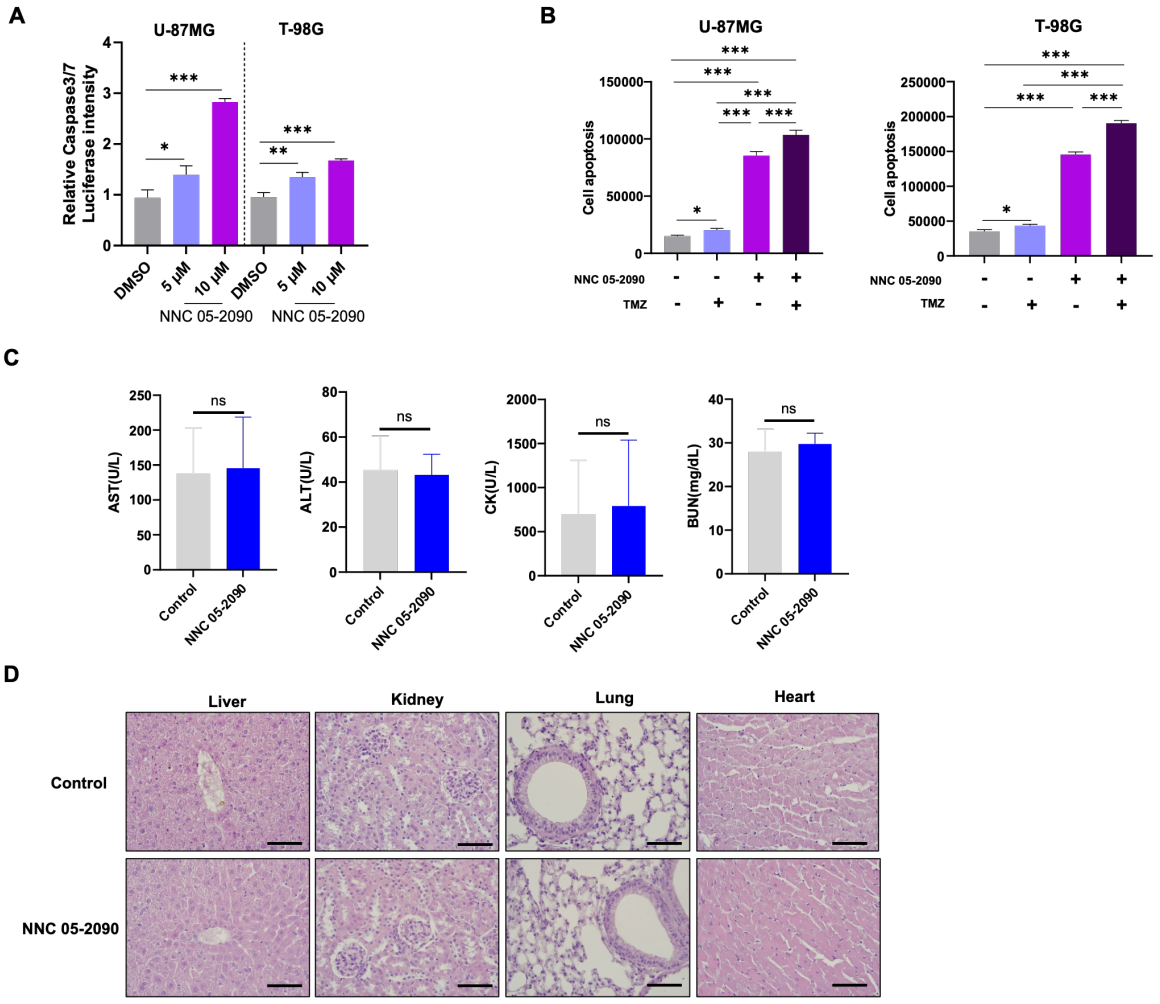

Figure S7. Cell apoptosis analysis in glioma cells and serum chemistry and histopathological analysis in control and NNC 05-2090-treated mice.

A. Cell apoptosis in glioma cell lines treated with the indicated concentrations of NNC 05-2090. Cell apoptosis was assessed by Caspase-Glo 3/7 assay. B. Cell apoptosis in U-87MG (left) and T-98G (right) cells treated with NNC 05-2090 (10 μM), temozolomide (TMZ, 1 mM), or the combination of NNC 05-2090 and TMZ. Cell apoptosis was assessed by Caspase-Glo 3/7 assay. C. Serum levels of AST, ALT, CK, and BUN in control and NNC 05-2090-treated mice. Data are presented as mean ± SD. D. Representative H&E-stained sections of liver, kidney, lung, and heart from control and NNC 05-2090-treated mice. Scale bar, 50 μm. AST, aspartate transaminase; ALT, alanine transaminase; CK, creatine kinase; BUN, blood urea nitrogen. Data are presented as means ± SD (*$P < 0.05$, **$P < 0.01$, ***$P < 0.001$).

Supplementary Table S1. List of sequences

	Gene	Primer (Sense)	Primer (antisense)
NMUR2 CDS primers	NMUR2	TTTGAATTCGCCACCATGTCAGGGATGGAA	GTTCCGCGGTCAGGTTTTGTTAAGTGGAA
siRNA sequences	Negative control siRNA (siNC)	UUCUCCGAACGUGUCACGUTT	ACGUGACACGUUCGGAGAATT
	siNMUR2-1	AGAAUGCUUCCUGGAUCUA	UAGAUCCAGGAAGCAUUCU
	siNMUR2-2	GCUGACCGAAGAUAUAGGU	ACCUAUAUCUUCGGUCAGC
qPCR primers	GAPDH	CTCTGCTCCTCCTGTTCGAC	TTAAAAGCAGCCCTGGTGAC
	NMUR2	AGATGTGGCGCAACTACCC	CGAAGCACACGGTCTCAAAGA
	PIM1	GAGAAGGACCGGATTTCCGAC	CAGTCCAGGAGCCTAATGACG
	FOXM1	ATACGTGGATTGAGGACCACT	TCCAATGTCAAGTAGCGGTTG
	Cyclin D1	GCATGTTCGTGGCCTCTAAG	CGTGTTTGCGGATGATCTGT
	Cyclin B1	TGAGGAAGAGCAAGCAGTCA	CCAAATGCGTGTCCTCAGAG
	CDKN 1B	GCAAGTACGAGTGGCAAGAG	CCAAATGCGTGTCCTCAGAG
Promoter assay	PIM1	GGCCGGTACCTGAGCTCGCTAGCGTGAAAACTGGTTAAATCAAGCGCAC	CGAGGCCAGATCTTGATATCCTCGAGGGAGTGGAGGAGTCAGGCCTGGAACAGAAC
	FOXM1	GGCCGGTACCTAGCTCGCTAGCGTCTGTGCCCCTCTTCCAGGATTGGGCTG	CGAGGCCAGATCTTGATATCCTCGAGGAACGATCGTCTGCTCCCCCCGATTAG
NMUR2 Tango sequences	NMUR2 optimized sequences	ATGTCCGGGATGGAAAAACTTCAGAACGCCAGTTGGATTTACCAACAGAAGCTGGAGGATCCTTTCCAGAAGCACCTGAACTCTACAGAGGAATACCTGGCTTTCCTCTGCGGCCCAAGACGATCCCACTTCTTTTTGCCCGTGTCAGTCGTGTACGTGCCCATTTTTGTGGTCGGCGTCATAGGGAACGTGCTTGTGTGCCTGGTTATTCTGCAGCATCAGGCCATGAAAACTCCAACAAATTATTACCTCTTTAGTCTGGCAGTGTCTGATCTGCTCGTGCTTCTGTTGGGCATGCCTCTGGAGGTATACGAGATGTGGAGAAATTATCCTTTTCTGTTTGGCCCCGTGGGTTGTTACTTCAAGACTGCTCTTTTTGAGACCGTCTGTTTCGCTTCCATCCTCAGCATAACGACAGTGTCTGTGGAACGCTATGTCGCCATCCTGCACCCATTTCGAGCTAAGCTGCAATCCACCCGCCGGCGGGCCCTCAGAATTCTGGGCATCGTGTGGGGCTTCTCAGTTCTGTTTTCCCTGCCAAATACTAGTATTCATGGAATTAAATTTCATTACTTTCCTAATGGGTCCCTTGTGCCCGGCTCTGCCACATGCACCGTTATTAAGCCTATGTGGATCTACAACTTCATTATCCAAGTCACAAGTTTTTTGTTCTACCTGTTGCCGATGACAGTTATATCAGTACTGTACTACCTCATGGCCCTGCGGCTGAAAAAAGACAAAAGCCTTGAGGCAGATGAGGGGAATGCCAACATCCAGCGCCCTTGTCGCAAATCTGTGAACAAGATGCTTTTTGTGTTGGTACTGGTTTTTGCTATTTGCTGGGCCCCATTCCACATTGACCGGCTGTTTTTTTCTTTTGTCGAGGAATGGTCTGAAAGCCTTGCTGCCGTGTTCAACCTGGTGCACGTCGTTTCAGGCGTATTCTTTTATCTGTCCTCCGCCGTTAATCCTATAATTTACAATCTGCTTAGCAGAAGATTCCAGGCTGCATTCCAGAATGTAATCTCATCATTTCACAAACAGTGGCATAGTCAGCACGACCCCCAGCTCCCACCGGCTCAGAGAAATATCTTTCTCACGGAGTGCCACTTCGTGGAACTCACCGAAGATATCGGGCCGCAGTTTCCCTGTCAGTCTTCAATGCACAATAGCCACCTGCCTGCCGCCCTGAGTAGCGAGCAGATGTCCCGGACTAACTATCAGTCCTTCCACTTCAATAAGACG